A&A 493, 471–479 (2009)
DOI: 10.1051/0004-6361:200810550

Astronomy & Astrophysics

New period-luminosity and period-color relations of classical Cepheids

III. Cepheids in SMC

A. Sandage[1], G. A. Tammann[2], and B. Reindl[2]

[1] The Observatories of the Carnegie Institution of Washington, 813 Santa Barbara Street, Pasadena, CA 91101, USA
[2] Department of Physics and Astronomy, Univ. of Basel Klingelbergstrasse 82, 4056 Basel, Switzerland
e-mail: g-a.tammann@unibas.ch

Received 9 July 2008 / Accepted 13 October 2008

ABSTRACT

The photometric data for 460 classical, fundamental-mode Cepheids in the SMC with $\log P > 0.4$ measured by Udalski et al. have been analyzed for their period-color (P–C) and period-luminosity (P–L) relations, and for the variation in amplitude across the instability strip in a similar way to what was done in Papers I and II of this series. The SMC Cepheids are bluer in $(B-V)^0$ at a given period than for both the Galaxy and the LMC. Their P–C relation in $(B-V)^0$ is best fit by two lines intersecting at $P = 10$ days. Their break must necessarily exist also in the P–L relations in B and/or V, but it remains hidden in the magnitude scatter. An additional pronounced break of the P–L relations in B, V, and I occurs at $P = 2.5$ days. The observed slope of the lines of constant period in the HR diagram agrees with the theoretical expectation from the pulsation equation. The largest amplitude Cepheids for periods less than 13 days occur near the blue edge of the instability strip. The sense is reversed in the period interval from 13 to 20 days, as in the Galaxy and the LMC. The SMC P–L relation is significantly flatter than that for the Galaxy, NGC 3351, NGC 4321, M31, all of which have nearly the same steep slope. The SMC P–L slope is intermediate between that of these steep slope cases and the very shallow slope of Cepheids in the lower metallicity galaxies of NGC 3109 and Sextans A/B, consistent with the premise that the Cepheid P–L relation varies from galaxy-to-galaxy as a function of metallicity. Failure to take the slope differences in the P–L relation into account as a function of metallicity using Cepheids as distance indicators results in incorrect Cepheid distances. Part of the 15% difference between our long distance scale – now independently supported by tip of the red-giant branch (TRGB) distances – and that of the HST Key Project short scale is due to the effect of using an inappropriate P–L relation.

Key words. stars: variables: Cepheids – galaxies: Magellanic Clouds – cosmology: distance scale

1. Introduction

The Galaxy, the LMC, and the SMC are the only three galaxies that have reddenings for their Cepheids that are determined by a method that is independent of using a fiducial Cepheid period-color relation that is incorrectly assumed to be universal. Once reliable reddenings are available by such independent methods, and by using data for galaxies where the reddening can be assumed to be nearly zero, differences in the slope and zero points of P–L relations in different galaxies as a function of metallicity follow from the observations (Tammann et al. 2008, hereafter TSR 08a, see their Fig. 4.; Sandage & Tammann 2008, hereafter ST 08, Fig. 4).

In Paper I of this series (Tammann et al. 2003, hereafter TSR 03) we analyzed the CCD photometric data by Berdnikov et al. (2000) for 321 Cepheids in the Galaxy for this purpose. A preliminary comparison of the P–L and P–C relations for the Cepheids in the LMC (593 stars) and SMC (459 stars) was also given there using the CCD photometry by Udalski et al. (1999a,b).

In Paper II (Sandage et al. 2004, hereafter STR 04) the lines of constant period that thread the instability strip were derived for the LMC by correlating the residuals in magnitude at fixed period read from the P–L relation with those from the P–C relations for individual Cepheids. We also derived the difference in the slopes and zero points of the ridge-lines of the instability strip (i.e. the $\log L$, $\log T_e$ HR diagram) for the Galaxy and the LMC, showing that Cepheids in LMC are hotter at a given luminosity by about 300 K at $\log L = 3.5$ (Fig. 20 of STR 04), but the size of the difference varies with period (Fig. 3 of STR 04) because of the slope difference in the two instability strips.

The purpose of the present paper is to continue with a similar study for the SMC using the data of Udalski et al. (1999b). The plan of the paper is this. The period-color relations in $(B-V)^0$ and $(V-I)^0$ for SMC in Sect. 2 are similar to Fig. 6 of TSR 03 but with more detail, showing the difference in the P–C relations between the Galaxy and SMC and emphasizing the break at 10 days for SMC. The slope of the SMC P–L relation in Sect. 3 is significantly flatter than those for the Galaxy and LMC, similar to Fig. 14b of TSR 03. Lines of constant period in the HR diagram for SMC are derived in Sect. 4. The slopes are compared there with that expected from the pulsation equation. Section 5 shows the correlation of amplitude with position in the instability strip for various period and absolute magnitude ranges. The SMC instability strip in M_V, $(B-V)^0$ and $(V-I)^0$, with and without the break at 10 days, and the resulting $\log L_V - \log T_e$ instability strip is in Sect. 6. Comparison of the SMC P–L relation with those in the high metallicity galaxies of NGC 3351, NGC 4321 (with slopes that are nearly identical to the P–L slope for the Galaxy) and the low metallicity galaxy NGC 3109 is in Sect. 7 showing the significant difference in the P–L slope as

function of metallicity and therefore that the P–L relation is not universal from galaxy to galaxy.

2. Comparison of the P–C and color–color relations for the Galaxy and SMC

2.1. Observational data

In the framework of the OGLE program, Udalski et al. (1999b) have observed *UBVI* magnitudes of over 2000 variables in 11 strips covering much of the central parts of SMC (see their Fig. 1). The magnitudes were corrected for absorption using reddening values of adjacent red-clump stars. Their adopted reddening-to-absorption ratios are the same for all practical purposes as those used by STR 04. The authors derived intensity-averaged mean magnitudes as well as periods where possible. The light curves in I are exceptionally well defined by several hundred epochs; the B and V light curves rest on 15–40 epochs which is sufficient in almost all cases. The authors have derived also light curve amplitudes and Fourier coefficients R_{21} and Φ_{21}. These parameters allowed a convincing separation of classical Cepheids from population II Cepheids and other variables and to subdivide the classical Cepheids in 1216 fundamental and 833 overtone pulsators.

About half of the fundamental-mode Cepheids have periods shorter than $\log P = 0.4$ ($P < 2.5$ days). This great abundance of short-period Cepheids is specific for SMC with its very low metallicity of $[O/H]_{T_e} = 7.98$ (Sakai et al. 2004). Some such Cepheids are known in other metal-poor galaxies, but they are rare in young populations with higher metallicity as for instance in LMC. The light curve parameters like magnitude, color, amplitude, and Fourier coefficients of the short-period Cepheids in SMC are continuous extensions of those with longer periods. Therefore they are most likely classical populations I Cepheids (see also Bauer et al. 1999; Sharpee et al. 2002), although taken as a whole they lie below the extrapolated P–L relation defined by the longer-period Cepheids and they are bluer than the extrapolated P–C relation defined by the latter. The proliferance of short-period Cepheids in SMC was explained by Becker et al. (1977) as the effect of the evolutionary loops of low-mass red giants extending deeper to the blue side of the CMD, and hence still crossing or at least penetrating the instability strip, if the metallicity decreases. The dependence of the loop size on metallicity was first found by Hofmeister (1967).

In the following we are not concerned with the SMC Cepheids with $\log P < 0.4$ because our emphasis lies on the difference of Cepheids from galaxy to galaxy and on the ensuing effect on distance determinations. For this purpose the short-period Cepheids are not helpful because statistically meaningful samples of Cepheids with $\log P < 0.4$ are not available in other galaxies. Therefore only SMC Cepheids with $\log P > 0.4$ are considered in the following.

The sample of fundamental-mode SMC Cepheids with $\log P > 0.4$ was cleaned by Udalski et al. (1999b) by removing all objects deviating by 2.5σ or more from a common P–L relation. This left 469 Cepheids with V magnitudes. We have removed some additional outliers resulting in 460 Cepheids with V and I magnitudes, of which 439 objects have also B magnitudes. Their data are the basis of the following analysis.

2.2. The period-color relation

We adopt the individual reddenings for the SMC Cepheids derived by Udalski et al. (1999b) determined from the observed color of the red clump stars in the vicinities of the Cepheids. It is important to note that these reddenings have been determined by a method that is independent of using some adopted fiducial P–C relation. Because the P–C color relation varies with metallicity at the 0.2 mag level, it is necessary to determine its slope and zero point for every specific metallicity. Systematic errors in the calculated reddenings will be made if a fixed "universal" fiducial P–C relation is used in galaxies with metallicities that differ from that of the fiducial sample.

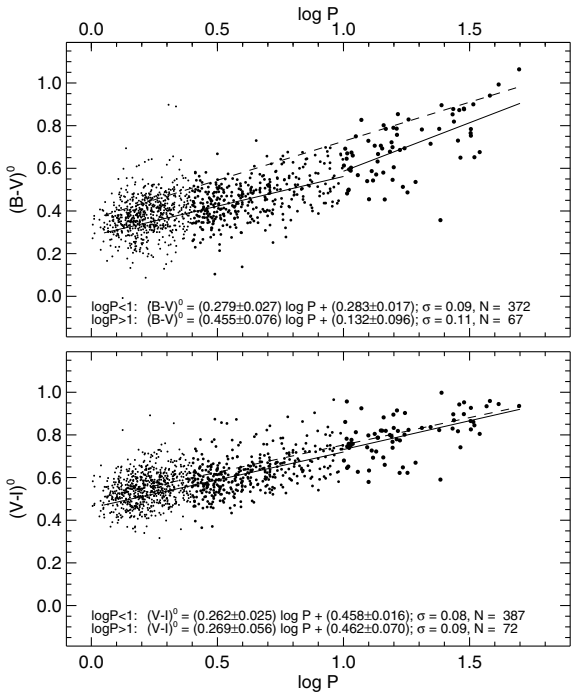

Fig. 1. The SMC period-color relations in $(B-V)^0$ and $(V-I)^0$. Small dots are for $\log P < 0.4$. Large dots are for $\log P > 1.0$, separated at this period to emphasize the break at that period. The least squares equations for $\log P > 0.4$ and assuming a break at 10 days (solid lines) are listed inside the diagram. The P–C relations for the Galaxy (no-break) are the dashed lines taken from Eqs. (3) and (4). The period-color relations for the LMC (not shown) are intermediate between the Galaxy and the SMC as given by Eqs. (2) and (3) for $(B-V)^0$ and Eqs. (5) and (6) for $(V-I)^0$ in STR 04.

Least-squares solutions of the $(B-V)^0$ and $(V-I)^0$ colors of all Cepheids with $\log P > 0.4$ selected from the SMC sample of Udalski et al. yield

$$(B-V)^0 = (0.360\pm0.016)\log P + (0.235\pm0.012), \sigma = 0.09, \quad (1)$$
$$(V-I)^0 = (0.276\pm0.014)\log P + (0.450\pm0.010), \sigma = 0.08. \quad (2)$$

(Flatter slopes for SMC are shown in Table 4 of TSR 08a, but they do actually include also the many Cepheids with $\log P < 0.4$).

For comparison the Galactic P–C relations for $\log P > 0.4$ are repeated here from TSR 03 (the update here in the equations for the Galaxy compared with the Galactic equations in TSR 03 and STR 04, obtained by subtracting Eqs. (16)–(18) there, is insignificant for this comparison):

$$(B-V)^0 = (0.366\pm0.015)\log P + (0.361\pm0.013), \sigma = 0.07, \quad (3)$$
$$(V-I)^0 = (0.256\pm0.017)\log P + (0.497\pm0.016), \sigma = 0.07. \quad (4)$$

The P–C relations of SMC and the Galaxy have quite similar slopes above $\log P = 0.4$, but the striking difference is that the SMC Cepheids are bluer by $\Delta(B-V)^0 = 0.13$

and $\Delta(V-I)^0 = 0.03$ than the Galactic ones. This was discovered already by Gascoigne & Kron (1965; see also Gascoigne 1974) and made definitive by Laney & Stobie (1986, 1994) as a temperature difference.

The individual Cepheids defining the SMC P–C relations of Eqs. (1) and (2) are plotted in Fig. 1. Here the $(B-V)^0$ data strongly suggest that a single-slope P–C relation does not provide an optimum fit, but that the slope changes around $\log P \sim 1$. Two separate fits for the period intervals $\log \gtrless 1$ lead for $0.4 < \log P < 1$ to

$$(B-V)^0 = (0.279 \pm 0.027)\log P + (0.283 \pm 0.017),\ \sigma = 0.09, \quad (5)$$

and for $\log P > 1$ to

$$(B-V)^0 = (0.455 \pm 0.076)\log P + (0.132 \pm 0.096),\ \sigma = 0.11. \quad (6)$$

The change of slope has here a significance of 2σ. The case is reminiscent of LMC where the break at $P = 10^{\rm d}$ is well documented. In both galaxies the long-period Cepheids have a steeper color gradient than at shorter periods.

For the sake of completeness we also give the separate SMC P–C relations in $(V-I)^0$ for the period interval $0.4 < \log P < 1$:

$$(V-I)^0 = (0.262 \pm 0.025)\log P + (0.458 \pm 0.016),\ \sigma = 0.08, \quad (7)$$

and for $\log P > 1$:

$$(V-I)^0 = (0.269 \pm 0.056)\log P + (0.462 \pm 0.070),\ \sigma = 0.09. \quad (8)$$

They turn out to be statistically undistinguishable. Their slope is also quite close to the Galactic slope in Eq. (4).

A comparison of the Galactic P–C relation in $(B-V)^0$ in Eq. (3) with the corresponding SMC P–C relations in Eqs. (5) and (6) reveals a slope difference, both above and below the 10 day break. It will be shown in Sect. 5 that these slope differences translate into slope differences in temperature in the $M_V - \log T_{\rm e}$ instability strip diagram (Figs. 8 and 9 later).

2.3. Proof via the $(B-V)^0$, $(V-I)^0$ color–color diagram that the intrinsic color difference between SMC and the Galaxy is real

The validity of the color differences between the Galaxy and SMC in Fig. 1 depends, of course, on the accuracy of the reddening determinations for both the Galaxy and the SMC. One might suppose that the observed color difference in Fig. 1 is not real because of errors in the reddenings, although the methods used by Fernie (1990, 1994) and Fernie et al. (1995) are very powerful. However, this possibility can be disproved by appeal to the $(B-V)^0$, $(V-I)^0$ color-color diagram for SMC compared with that for the Galaxy shown in Fig. 7a of TSR 03. There is an offset in that diagram of ~0.1 mag in $(B-V)^0$ at a given $(V-I)^0$, with SMC Cepheids being bluer than those in the Galaxy. Because the reddening line is nearly parallel to the observed correlation line (Panel a of Fig. 7a of TSR 03), errors in the reddenings will not produce the observed color offsets seen in Panel c. Furthermore, the observed offset of SMC relative to the Galaxy is close to what is expected from model atmosphere calculations by Bell & Tripicco from Table 6 of Sandage et al. (1999, hereafter SBT 99), shown in Panel d of Fig. 7a in TSR 03. Hence, the color offset in Fig. 1 here of SMC relative to the Galaxy is not due to reddening errors, but is real.

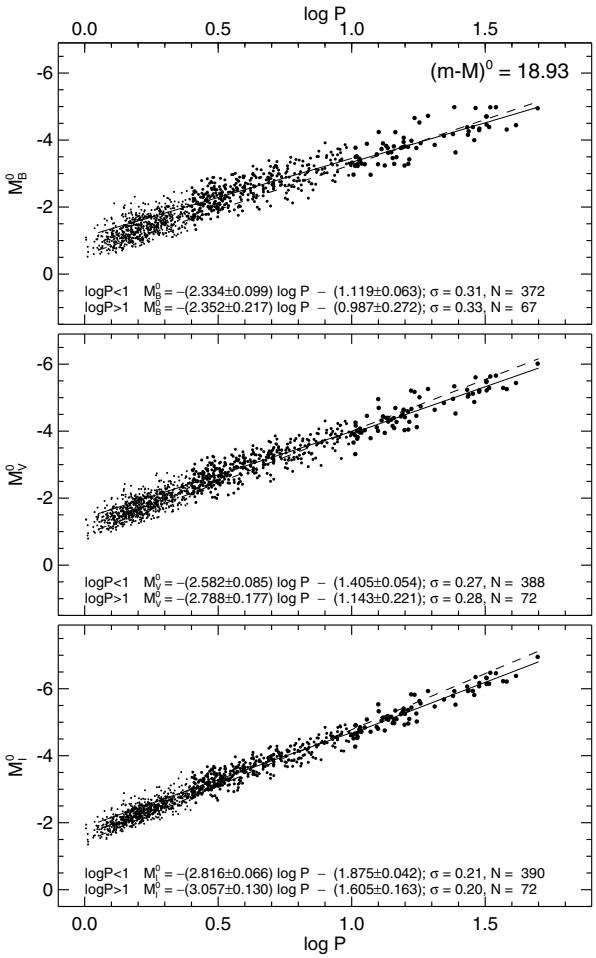

Fig. 2. The P–L relations in B, V, and I for the SMC from the absorption corrected data of Udalski et al. (1999b). The different symbols for $\log P < 0.4$ and $\log P > 1.0$ are the same as in Fig. 1. The least-squares solutions for $0.4 < \log P < 1.0$ and $\log P > 1.0$, assuming a break at $10^{\rm d}$ (solid lines) are listed inside the diagram. The P–L relations for the Galaxy from Eqs. (16)–(18) of STR 04 are shown for comparison as the dashed line in each panel.

3. The SMC P–L relation compared with the Galaxy and the LMC

The SMC P–L relations in B, V, and I from the data by Udalski et al. (1999b) are shown in Fig. 2, using a zero point for the SMC distance modulus of $(m-M)^0 = 18.93$ taken from a summary given elsewhere for modulus values determined after 2004 (TSR 08a, Table 7). The symbols are the same as in Fig. 1.

Least squares solutions for the ridge-line P–L equations were made with and without a break at 10 days using Cepheids with $\log P > 0.4$. This period restriction is to make the comparison here with LMC more secure where the same period cut-off was used. The break equations are shown within the borders of Fig. 2. The non-break equations are

$$M_B^0 = -(2.222 \pm 0.054)\log P - (1.182 \pm 0.041),\ \sigma = 0.31 \quad (9)$$

$$M_V^0 = -(2.588 \pm 0.045)\log P - (1.400 \pm 0.035),\ \sigma = 0.27 \quad (10)$$

$$M_I^0 = -(2.862 \pm 0.035)\log P - (1.847 \pm 0.027),\ \sigma = 0.21. \quad (11)$$

The break is less significant for SMC Cepheids than in the LMC.

The P–L relations for the Galaxy from Eqs. (16)–(18) of STR 04 are shown in Fig. 2 by the dashed line. The deviation of the SMC P–L relation from the Galaxy is clear. The SMC

Cepheids at $\log P = 0.4$ are ~0.2 mag brighter in V than those in the Galaxy at $\log P = 0.4$ and are ~0.3 mag fainter at $\log P = 1.5$. The difference is larger in B and smaller in I.

If one distrusts the Galaxy P–L slopes and zero points, either because of questions concerning main sequence fittings and problems with absorption (van Leeuwen et al. 2007) for star clusters and associations, or because of doubts about the reliability of the Baade/Becker/Wesselink moving atmosphere results due to an uncertainty on the velocity projection factor (Fouqué et al. 2007), comparison of the over-all slopes of the SMC P–L relations with those of the LMC again shows a difference, with the SMC slope being flatter in all three colors. The significance of the slope difference decreases from B to I. To avoid confusion, the LMC P–L relation is not overlayed in Fig. 2 to show this, but the LMC P–L Eqs. (7)–(9) of STR 04 differ significantly from the equations set out in Fig. 2 for SMC. The over-all SMC P–L relation compared with LMC is shown later in Fig. 10 in Sect. 7.

The comparison of the P–L relations of SMC and LMC becomes more complicated if one allows for the break at $P = 10^{\rm d}$. In the interval $0.4 < \log P < 1.0$ the SMC slopes are considerably *flatter* than those of LMC. The difference is again more pronounced in B than in I and intermediate in V. On the other hand the SMC slopes are *steeper* for $\log P > 1.0$ than those in LMC, the difference being about the same in all three colors.

A very tight P–L relation of SMC is obtained when the individual Cepheids are slid along the constant-period lines onto the ridge line of the P–L relation. The procedure is explained in TSR 08a (Eq. (3)) and the result is illustrated in Fig. 3b there. Because of the small dispersion of 0.15 mag the P–L relation is very well defined. The break at $\log P = 1$ is less pronounced than in LMC, but still has a significance of 2.3σ and is of opposite sign! Any claim that the P–L relations of LMC and SMC in Figs. 3a and 3b of TSR 08a were the same would be a denial of the evidence.

4. Lines of constant period in the SMC instability strip

4.1. Empirical determination from the data directly

Lines of constant period in the HR diagram thread from the luminous, high temperature upper left to the low luminosity, low temperature lower right. Therefore, Cepheids of a given period near the blue edge of the instability strip will be brighter than Cepheids near the red edge. Hence, there should be a correlation between luminosity residuals in the P–L diagram and the color residuals in the P–C diagram at fixed periods. The slope β of the constant-period lines in the instability strip in the $M, (B-V)^0$ plane is given by $\beta = \Delta M_{BVI}/\Delta(B-V)^0$.

The constant-period lines were well determined for the LMC, with average slopes of $\langle\beta_{B-V}\rangle = 1.8$ and $\langle\beta_{V-I}\rangle = 2.5$ and no significant variation with period (STR 04, Fig. 9 and Table 4). The same determination was made there for the SMC and is repeated here with the results shown in Fig. 3, binned in small intervals of period. The slopes at given period intervals are similar to those for LMC. The mean slopes over all periods are $\langle\beta_{B-V}\rangle = 1.8 \pm 0.2$ and $\langle\beta_{V-I}\rangle = 2.8 \pm 0.1$ for SMC.

4.2. Predicted slope of the constant period lines using the pulsation equation

The equation of the family of constant period lines in the $L_{\rm bol}, T_{\rm e}$ HR diagram follows from the $P(L, \text{mass}, T_{\rm e})$ pulsation equation when the mass is eliminated using a mass-luminosity relation for the Cepheids. It is shown elsewhere (ST 08) that the resulting equation for the family is

$$\log L_{\rm bol} = 5.472 \log T_{\rm e} + 1.572 \log P - 18.406. \quad (12)$$

Changing into a $M_V, (B-V)$ dependence by neglecting the bolometric correction (using the approximation that $M_{\rm bol} = M_V$, valid to ~0.1 mag over much of the color range of the Cepheids), and using a linearized $(V-I)$, temperature relation by interpolating in Table 6 of SBT 99 for the $\log g$ of Cepheids and with [A/H] = −0.7 for the SMC Cepheids gives

$$\log T_{\rm e} = -0.24(V-I) + 3.924, \quad (13)$$

over the range $0.5 < (V-I) < 0.9$. Substituting into Eq. (12) gives the equation of the constant period lines as,

$$M_V = 3.32(V-I) - 3.93 \log P - 2.92, \quad (14)$$

where we have used $M_V = -2.5 \log L + 4.75$.

The predicted slope here of 3.3 for the constant period lines in $V-I$ agrees well enough with the observed slope of 2.8 ± 0.1 considering the approximations we have made. A similar agreement obtains in $B-V$. These agreements to within the approximations show that the observed lines of constant period in Fig. 3 are understood as a consequence of the Ritter $P\sqrt{\rho}$ pulsation condition.

5. Correlation of amplitude with position in the instability strip

By analogy with the more easily visualized case of the RR Lyrae stars in globular clusters where the horizontal branch cuts the instability strip at nearly constant M_V, we make the same correlations for the Cepheids here as is the custom for globular cluster variables. The strong correlation of amplitude with strip position in globular clusters at fixed absolute magnitude (called now the Bailey diagram) shows that the largest amplitudes for RR Lyrae stars occur near the blue edge, decreasing monotonically toward the red edge.

However, the situation is more complicated for the Cepheids because there is no restriction in absolute magnitude as with the RR Lyrae stars. The absolute magnitude in V does not change appreciably for globular cluster variables, hence there is no period-luminosity relation in V. Of course, in other bands than V where the horizontal branch is not horizontal, there is a "pseudo" P–L relation caused however by the change of luminosity with color across the strip whereas for Cepheids the vertical change of absolute magnitude with period in the P–L strip is the principal effect.

Said differently, for RR Lyrae stars the principal parameters describing the fine structure of the instability strip are period, color, and amplitude, not luminosity, whereas for Cepheids the principal parameters are period and absolute magnitude, with color and amplitude having only a secondary role. It is the cutting of the strip by the horizontal branch in the globular clusters that restricts the way the parameters appear in the data.

The color-amplitude correlation for the RR Lyrae data is the striking feature of the data for the cluster variables. This translates into the more easily observed period-amplitude Bailey diagram which often dominates the RR Lyrae analyses. The correlation is less noticeable for the Cepheids because of the dominance of the overwhelming luminosity variation with period that is absent in the cluster variables.

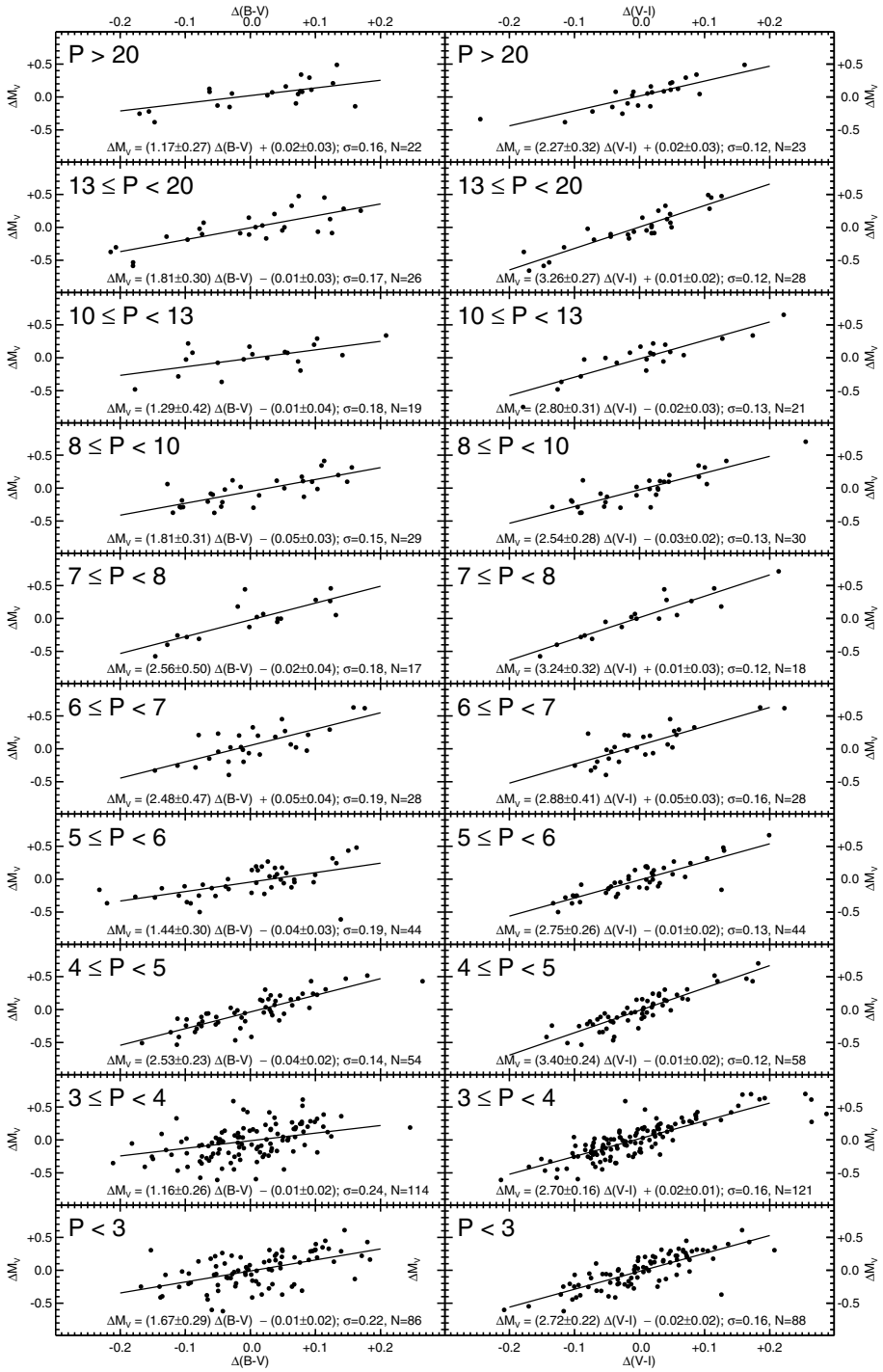

Fig. 3. The slope of the lines of constant period using the ratios of the residuals in $(B-V)^0$ and $(V-I)^0$ from the P–C relations of Fig. 1, and the magnitude residuals from Fig. 2 for the Cepheids in SMC in the period intervals indicated. The sense of the correlations is that Cepheids near the blue border of the instability strip are intrinsically brighter than those near the red border.

Nevertheless there is a color-amplitude effect at fixed period (or fixed absolute magnitude) for the Cepheids, with the highest amplitude Cepheids occurring at the blue edge of the strip, just as for the RR Lyrae stars, at least in the period range from 3 to 10 days in the LMC (STR 04, Fig. 11) with the trend reversing for periods from 10 to 20 days, and perhaps returning again to high amplitudes at the blue edge for $P > 20$ days (STR 04, Fig. 11). The effect was seen initially in the Galaxy where the reversal of the sense occurs at $\log P = 0.86$, and returns to the original sense for $\log P > 1.3$. This result was originally suggested from a small sample of Galaxy Cepheids (Sandage & Tammann 1971), and was confirmed in STR 04 (Sect. 6.3) from the much larger sample of Galaxy Cepheids in the Berdnikov et al. (2000) sample.

The effect was shown to be the same for the LMC Cepheids in the period range from 3 to 10 days and for $P > 20$ days, and again the sense is reversed for $10 < P < 20$ days (STR 04, Figs. 11 and 12).

We have analyzed the large data sample for the SMC in the same way, with the results shown in Figs. 4 and 5. The sense of the trends are identical with those in the Galaxy and LMC. The reversal of the sense for periods between 10 and 20 days is also evident here for the SMC although the period range is different. For SMC the reversal occurs between 13 and 20 days, while in the Galaxy it is between 7 and 20 days and for the LMC it is between 10 and 20 days. The absolute magnitude range for the change of sense is almost identical in each case at

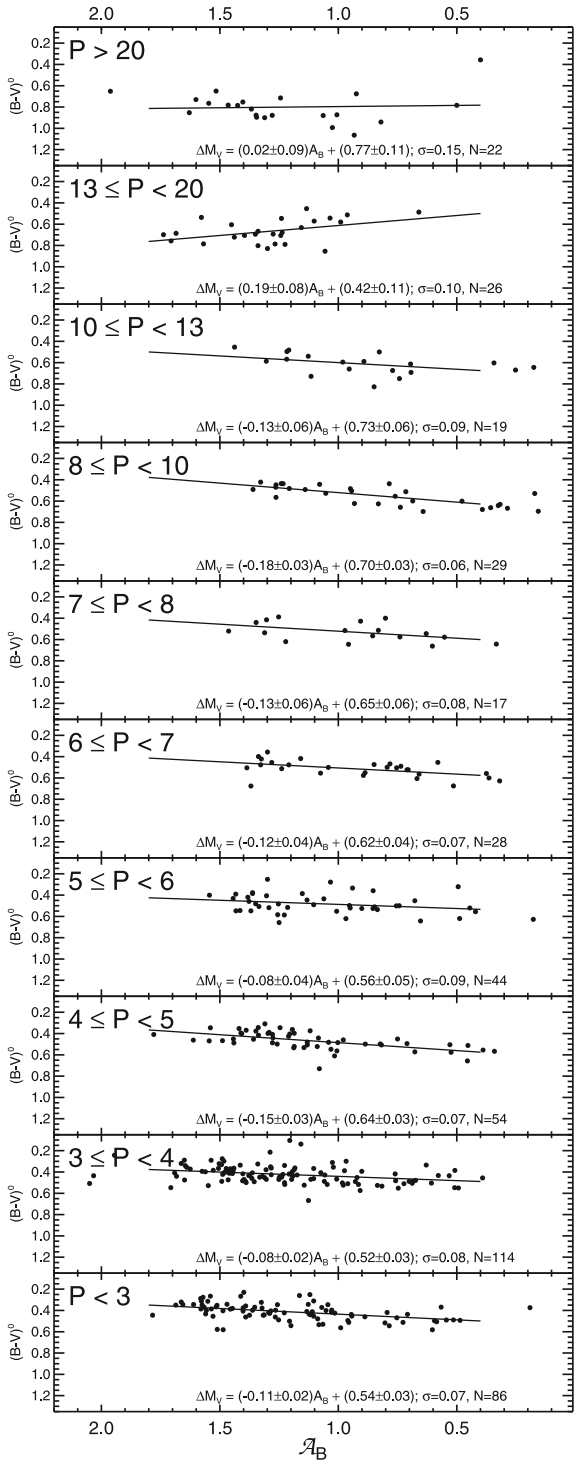

Fig. 4. Correlation of B band amplitude with color for SMC Cepheids in various period ranges, showing that the largest amplitude variables are near the blue edge of the instability strip except in the period range $13 < P < 20$ days.

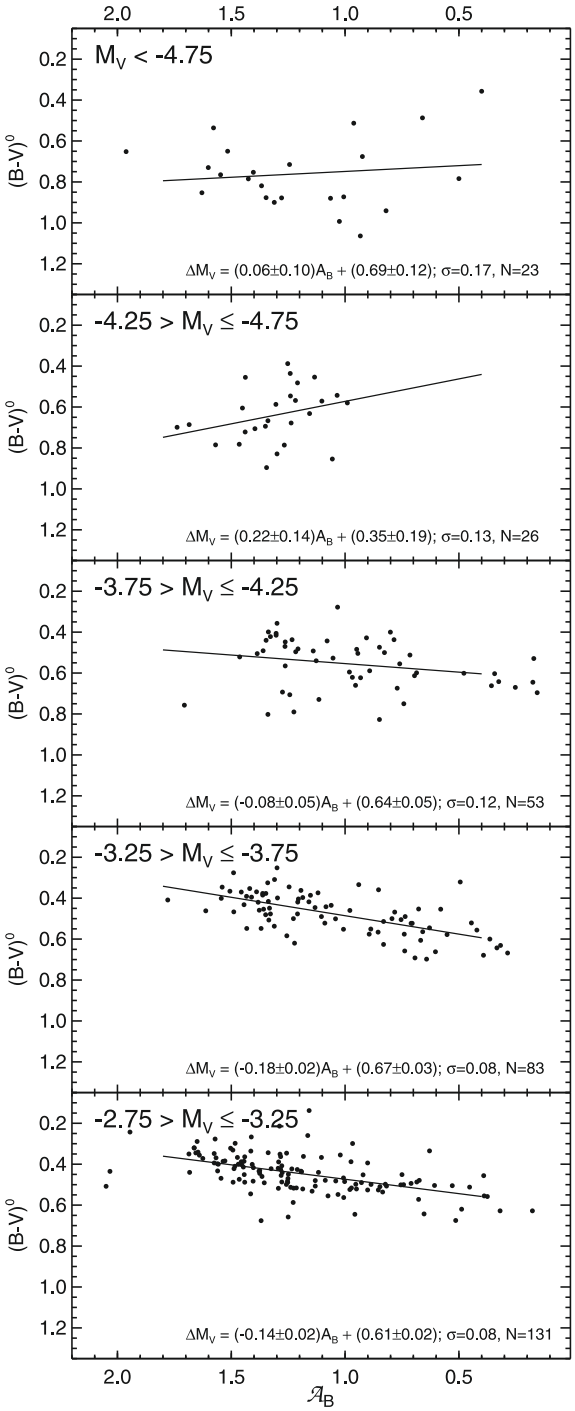

Fig. 5. Same as Fig. 4 but binned in absolute magnitude intervals rather than period intervals. The reversal in the sense of the correlation of amplitude with color for the absolute magnitude interval near $M_V \sim -4.5$ is the same as in the LMC.

between M_V of −4.25 and −4.75. The reason for this behavior is not yet understood.

Because the amplitudes are largest at the blue edge of the instability strip (except for the period range of 10 to 20 days), and because the blue edge of the strip is brighter than the red edge at fixed period (Fig. 3 here and Fig. 9 of STR 04 for LMC), there must be a period, magnitude, amplitude correlation in the sense that large amplitude Cepheids are brightest, seen in Eqs. (36)−(41) of STR 04. The maximum effect is at the level of ∼0.2 mag, and is a function of the "amplitude defect", a parameter introduced by Kraft (1960), calculated for each Cepheid from the deviation of a given amplitude from the upper envelope line of the period-amplitude relation. The bias effect on distances and the severity of the effect for the extragalactic distance scale is small as discussed in detail in STR 04, Sect. 6.3, and is not repeated here. Nevertheless, the existence of the effect leads to the notion of fine structure in the P−L relation depending on amplitude, and is to be discussed separately elsewhere.

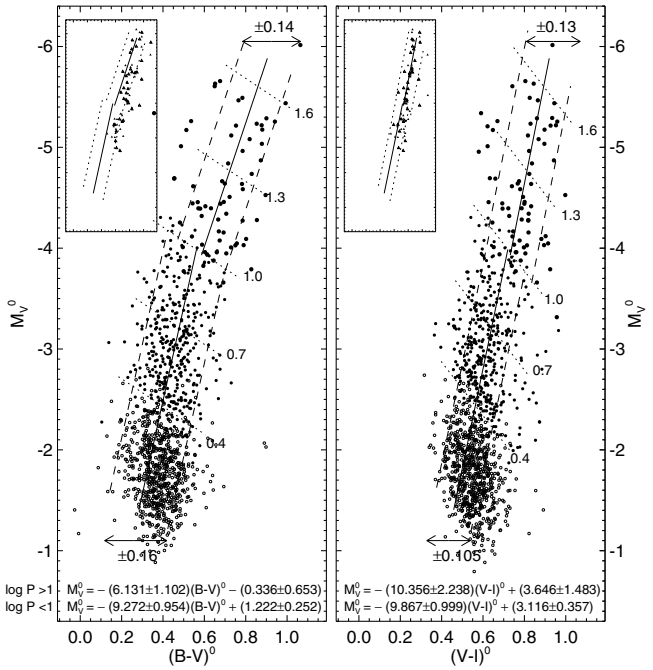

Fig. 6. The Cepheid instability strip for the SMC Cepheids in the M_V-color plane allowing for a break at 10 days (see text). Variables with periods less than $\log P = 0.4$ are shown as small open circles. Five lines of constant period are drawn and marked by their $\log P$ values. The insert diagrams repeat the ridge line equations for SMC. The 53 individual Cepheids in the Galaxy from the data in TSR 03 and STR 04 are shown as points in the inserts. The significant blueward offset of the SMC Cepheids in the $(B-V)^0$ insert panel is evident.

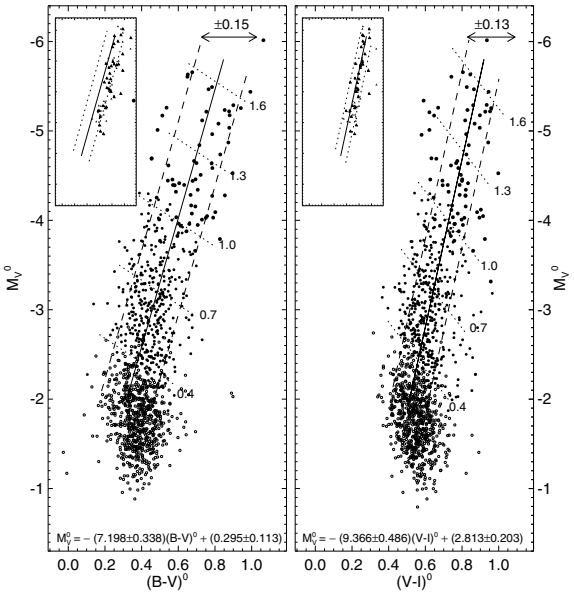

Fig. 7. Same as Fig. 6 but the ridge-line solutions are made with no break at 10 days. The insert diagrams again emphasize the difference in the instability strips in SMC (solid lines) compared with the Galaxy (individual points) in both slope and zero point.

6. SMC instability strip in color and in T_e

6.1. The magnitude–color instability strip

The instability strip in M_V vs. $(B-V)^0$ and $(V-I)^0$ for the SMC Cepheids is in Fig. 6. The ridge line equations with a break at 10 days, shown at the bottom of Fig. 6, are obtained by substituting the $\log P$ term in the P–L relations at the bottom of Fig. 2 by means of the P–C relations given in Eqs. (5)–(8). The ridge lines are shown as full lines in Fig. 6. The break is suggestive in the $(B-V)^0$ panel but is not as pronounced in $(V-I)^0$. The blue and red edges of the strip, shown as dashed lines, are put parallel to the ridge lines using widths of 0.16 and 0.105 mag, respectively, for $P < 10^d$ and 0.14 and 0.13 mag for $P > 10^d$. These values are derived from the calculated rms spreads in the P–L relations in Fig. 2 and the mean slopes of the lines of constant period from Sect. 4. The lines of constant period are shown for $\log P$ of 0.4, 0.7, 1.0, 1.3 and 1.6 using the formulation in Sect. 4.

The insert diagrams in Fig. 6 repeat the ridge-line equations and are shown as the solid lines with the edges of the instability strip also repeated. The individual points in the inserts are the 53 Cepheids in the Galaxy sample taken from Tables 3 and 4 of TSR 03, as updated in STR 04, Sect. 4.2. The difference in the SMC ridge lines and the position of the Cepheids in the Galaxy, is evident. This difference is the same as seen in Fig. 1 but in a different representation.

Figure 7 is the same as Fig. 6 but with no allowance for the break at 10 days, i.e. the P–L relations in Eqs. (9)–(11) were combined with the P–C relations in Eqs. (1) and (2) to yield the no-break ridge line equations at the bottom of Fig. 7. Again, the differences in the slope and the zero point of the instability strip ridge lines for SMC compared with the Galaxy Cepheids (the individual points) are evident in the insert diagrams.

6.2. The instability strip in log L_V vs. log T_e

The data in Figs. 6 and 7 have been transformed to the $\log L_V$, $\log T_e$ representation of the instability strip in the same way as we did for the Cepheids in LMC in Fig. 20 of STR 04. The $(B-V)^0$ and $(V-I)^0$ colors are changed into $\log T_e$ by interpolations in Table 6 of SBT 99 using appropriate $\log g$ values as function of period[1] (from the P–L relation and the assumption of the Cepheid mass-luminosity relation), [A/H] metallicity values (0.0 for the Galaxy, −0.5 for LMC, and −0.7 for SMC), and a turbulent velocity of 1.7 km s^{-1}. The two values of $\log T_e$ for each Cepheid from the colors were averaged. We also assumed that the bolometric correction was small enough to be neglected in converting M_V to $\log L$ by $\log L_V = -0.4 M_V + 1.9$ (using $M_{bol}(\text{sun}) = 4.75$).

The results for the SMC break case are shown in Fig. 8. Those for the no-break solution are in Fig. 9. Also shown are the ridge-line solutions for the Galaxy (dot-dashed line) and the LMC (the heavy solid lines).

Both the SMC and the LMC ridge lines are at higher temperatures than the Galaxy line, and each have different slopes (except for LMC with $P < 10$ days where the ridge line is nearly parallel to that of the Galaxy). The consequences for these different slopes and zero points in the instability strips for differences in the slopes and zero points of the respective P–L relations are discussed in detail elsewhere (ST 08) and are not repeated here. However, the consequences for the P–L relation are shown graphically in the next section.

[1] $\log g = -1.09 \log P + 2.64$ as derived in STR 04 (Eq. (49)).

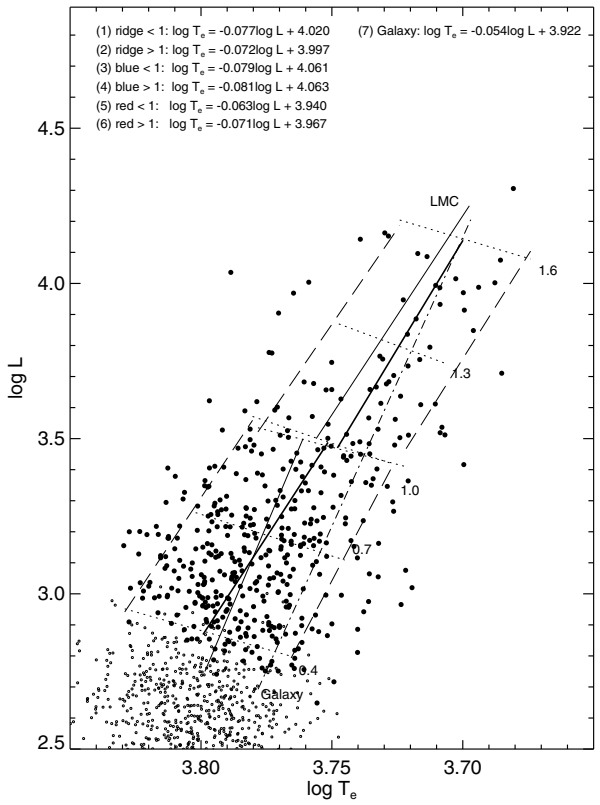

Fig. 8. The instability strip in log L_V, log T_e. The ridge-line relations for the Galaxy (dot-dashed line) and for the LMC and SMC with breaks at 10 days (solid lines). The individual SMC Cepheids are the dots. Cepheids with periods less than log $P = 0.4$ are the small open circles. The equation of the SMC ridge lines are in the upper left part of the diagram.

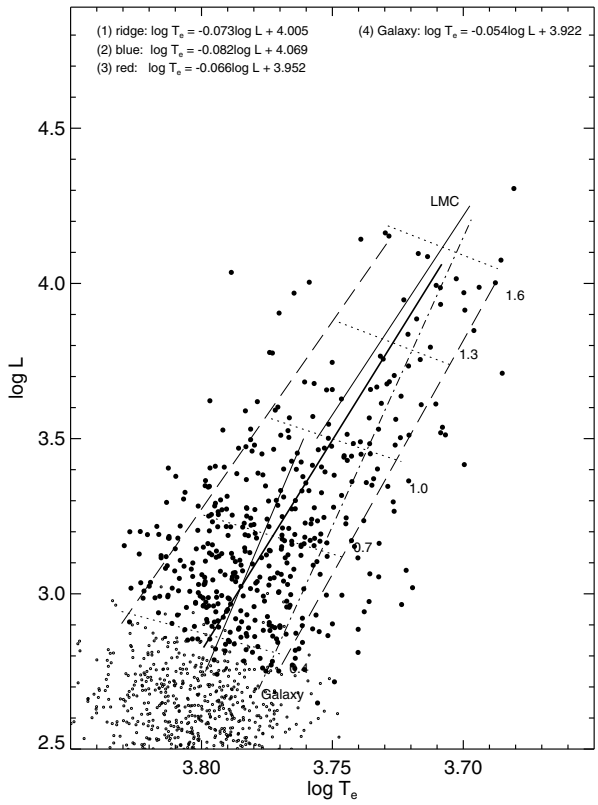

Fig. 9. Same as Fig. 8 but showing the no-break solution for the SMC.

7. SMC P–L relation compared with those in the Galaxy, NGC 3351 plus NGC 4321, the LMC, and NGC 3109

To emphasize that the data for a number of galaxies now support the proposition that the slopes of the Cepheid P–L relations differ from galaxy-to-galaxy as function of metallicity (low metallicity Cepheids have flatter P–L slopes), Fig. 10 shows a summary of the P–L relations of five galaxies (Galaxy, NGC 3351 plus NGC 4321, LMC, and NGC 3109) compared with the SMC here, illustrating the trend. More complete discussions are given elsewhere (TSR 08a, Table 5 and Fig. 4; ST 08, Fig. 4).

This diagram shows the importance of the SMC data because the difference between the Galaxy (or NGC 3351 plus NGC 4321) and the LMC is so small that a case made only using them is not convincing. However, the SMC P–L slope difference with LMC is large, and is supported more strongly when NGC 3109 is added.

The point to again be made is that the instability strip differences in slope of the ridge lines in Figs. 8 and 9 must show as a difference in the slopes of the P–L relations, as seen in Fig. 10. The case is supported because the instability strip data in Figs. 6–9 have not been used to obtain the slopes of the P–L relations in Fig. 10. These have been determined from the observational data alone using only periods and apparent magnitudes of the Cepheids in each galaxy.

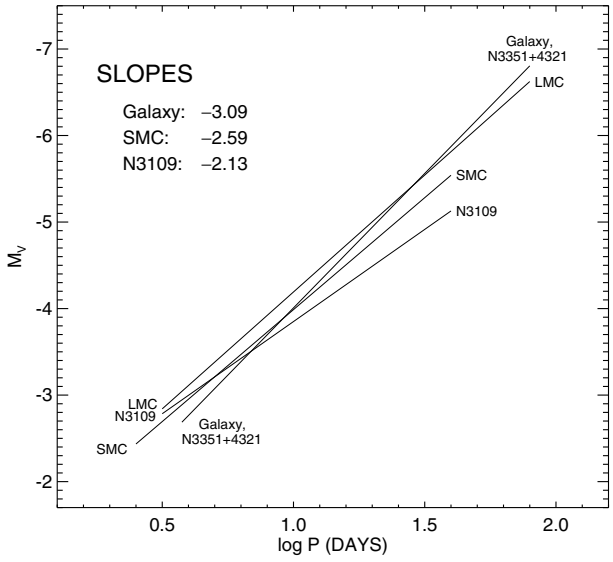

Fig. 10. Summary of the ridge lines of the P–L relations in 6 galaxies including the data analyzed here for the SMC. The slope differences are evident. They become flatter as the metallicity of the host galaxy becomes smaller. The P–L relations shown for SMC and LMC are single-fit solutions with no allowance for a break at $P = 10^d$.

8. Conclusions

The LMC and SMC are the two galaxies for which the largest numbers of classical Cepheids are known with excellent and consistent *BVI* photometry (Udalski et al. 1999a,b). They yield therefore particularly well to an intercomparison of their Cepheids, which is favored in addition by only small reddenings. The P–C and P–L relations of the Cepheids in the two galaxies, although sharing the change of slope at $P = 10$ days, are found to be significantly different in the overlapping period range of log $P > 0.4$. At least one parameter which governs these differences is the different metallicity of SMC ([O/H] = 7.98)

and LMC ([O/H] = 8.34) by a factor of 2.3. As confirmed also in other galaxies, metal-poor Cepheids are bluer than metal-rich Cepheids not only because of their weaker line blanketing effect, but also because of their higher temperature. In addition metal-poor Cepheids tend to be brighter at short periods and fainter at long periods than their Galactic counterparts. These differences are more pronounced at shorter wavelengths.

The P–L relation of SMC predicts fainter luminosities than that of LMC by about 0.2 mag. For distance determinations the effect is compensated or even overcompensated by the higher absorption attributed to the *blue* SMC Cepheids, such that a Cepheid sample with wide period coverage yields quite similar distances from the SMC or LMC P–C and P–L relations. The SMC distance, however, is *larger* at a period of 10 days by 0.1 mag. Of course, for still higher metallicities the difference can be larger for specific periods (see TSR 08b, Table 3).

Cepheid distances, consistently reduced as to metallicity and period, are compiled in TSR 08b, Table 2. The resulting "long" distance scale is in excellent agreement with the independent tip of the red-giant branch (TRGB) distance scale (TSR 08b), demonstrating the necessity of metal-dependent P–C and P–L relations if they are used for distance determinations.

The existence of a universal P–L relation of classical Cepheids is an only historically justified illusion (see also Romaniello et al. 2008).

Acknowledgements. We thank Dres. Alfred Gautschy and Francoise Combes for helpful informations and comments. A.S. thanks the Carnegie Institution for post retirement support facilities.

References

Bauer, F., Afonso, C., Albert, J. N., et al. (EROS Collaboration) 1999, A&A, 348, 175
Becker, S. A., Iben, I., Jr., & Tuggle, R. S. 1977, ApJ, 218, 633
Berdnikov, L. N., Dambis, A. K., & Voziakova, O. V. 2000, A&AS, 143, 211 (Galaxy)
Fernie, J. D. 1990, ApJS, 72, 153
Fernie, J. D. 1994, ApJ, 429, 844
Fernie, J. D., Beattie, B., Evans, N. R., & Seager, S. 1995, IBVS, 4148 http://www.astro.utoronto.ca/DDO/research/cepheids/cepheids.html
Fouqué, P., Arriagada, P., Storm, J., et al. 2007, A&A, 476, 73
Gascoigne, S. C. B. 1974, MNRAS, 166, 25
Gascoigne, S. C. B., & Kron, G. E. 1965, MNRAS, 130, 933
Hofmeister, E. 1967, Z. Astrophys., 65, 194
Kraft, R. P. 1960, ApJ, 132, 404
Laney, C. D., & Stobie, R. S. 1986, MNRAS, 222, 449
Laney, C. D., & Stobie, R. S. 1994, MNRAS, 266, 441
Romaniello, M., Primas, F., Mottini, M., et al. 2008, A&A, 488, 731
Sakai, S., Ferrarese, L., Kennicutt, R. C., & Saha, A. 2004, ApJ, 608, 42
Sandage, A., & Tammann, G. A. 1971, ApJ, 167, 293
Sandage, A., & Tammann, G. A. 2008, ApJ, 686, 779
Sandage, A., Bell, R. A., & Tripicco, M. J. 1999, ApJ, 522, 250
Sandage, A., Tammann, G. A., & Reindl, B. 2004, A&A, 424, 43 (STR 04)
Sharpee, B., Stark, M., Pritzl, B., et al. 2002, AJ, 123, 3216
Tammann, G. A., Sandage, A., & Reindl, B. 2003, A&A, 404, 423 (TSR 03)
Tammann, G. A., Sandage, A., & Reindl, B. 2008a, ApJ, 679, 52 (TSR 08a)
Tammann, G. A., Sandage, A., & Reindl, B. 2008b, A&ARv, 15, 289 (TSR 08b)
Udalski, A., Soszynski, I., Szymanski, M., et al. 1999a, AcA, 49, 223 (LMC)
Udalski, A., Soszynski, I., Szymanski, M., et al. 1999b, AcA, 49, 437 (SMC)
van Leeuwen, F., Feast, M. W., Whitelock, P. A., & Laney, C. D. 2007, MNRAS, 379, 723